A Computational Study on the Electronic Transport Properties of Ultranarrow Disordered Zigzag Graphene Nanoribbons

Nima Djavid, Kaveh Khaliji, Seyed Mohammad Tabatabaei, and Mahdi Pourfath, *Member, IEEE*

***Abstract*— In this paper, the effect of structural nonidealities on the electronic transport properties of ultranarrow zigzag graphene nanoribbons (ZGNRs) is systemically investigated for the first time, employing the nonorthogonal third nearest neighbor mean-field Hubbard model along with the nonequilibrium Green's function formalism. We have evaluated the influence of line-edge roughness, single atom vacancies, and substrate-induced potential fluctuations on the transport gap, ON- and OFF-state conductances, and the ON/OFF conductance ratio of 12-nm-length ultranarrow ZGNRs. The results reveal that while even moderate amounts of edge roughness lead to a nonuniform suppression of the transmission probability and increase the transport gap, the presence of single atom vacancies tends to decrease the induced transport gap. Furthermore, it is shown that the transport properties of ZGNRs are more robust against potential fluctuations compared with their armchair counterparts.**

***Index Terms*— Line-edge roughness (LER), mean-field Hubbard model, nonequilibrium Green's function (NEGF) formalism, single atom vacancy, substrate charged impurities, zigzag graphene nanoribbons (ZGNRs).**

I. Introduction

THE advent of graphene, a carbon-based material with atomic thickness and high carrier mobility, has heralded a new horizon in the quest for novel post-silicon materials [1]. However, the semimetal nature of pristine graphene imposes a serious obstacle regarding its potential application in digital logic circuits. This can be overcome by patterning graphene into quasi-1-D elongated strips, namely graphene nanoribbons (GNRs) [2]–[4]. Such structures are envisioned to be the key building blocks of a diverse range of future carbon-based devices. With the edge geometry, GNRs are categorized into armchair GNR (AGNR) or zigzag GNR (ZGNR). Compelling experimental evidence regarding the existence of localized edge states in ZGNRs, which leads to a peculiar type of magnetic ordering [5]–[8], renders zigzag-edged ribbons as suitable candidates for spintronic applications. Indeed, theoretical prediction of semiconducting to half-metallic transition in the presence of a transverse electric field and the realization of spin-valve devices based on ZGNRs with over 50% room temperature magnetoresistance are quite appealing in this respect [9], [10].

According to [11], at 12-nm technology node, for GNR-based field-effect transistors (FETs) to be an appropriate alternate for silicon-based FETs, bandgap of at least 0.4 eV and an ON/OFF current ratio as high as 10^4 are required. Owing to the inverse proportionality of the bandgap to the width in ZGNRs [12], only sub-2-nm-wide ribbons can meet the required projections. Nowadays, such narrow ribbons can be synthesized either by a chemical solution-based technique or a bottom-up self-assembly route starting from molecular precursors [2]–[4]. At these minute scales, sources of disorder may drastically impact the electronic performance, implying the necessity for evaluating the influence of relevant sources of disorder on the electronic transport properties of extremely narrow and ultrashort ZGNRs.

Extensive studies on the transport properties of AGNRs, in the presence of vacancies, edge and substrate-induced disorders have shown that moderate amounts of such nonidealities—which are inevitable in the state-of-the art fabrication processes—result in drastic reduction of linear conductance and induce large transport gaps causing semiconducting to Anderson insulator transitions [13]–[22]. These effects are more severe for ultranarrow AGNRs with a few number of propagating channels [20]. For ZGNRs, however, most of the previous works are either limited to wide ribbons where electron–electron interactions have a negligible effect on the electronic transport properties [13], [15], [17], [22] or mainly focus on the magnetic properties of defected ZGNRs [23]. In other studies, for performance assessment of ZGNR-based FETs, the presence of a specific case of nonidealities [15], [23], or a relatively few number of random realizations of disorder profile [15] are considered. For ZGNRs, in all the aforementioned studies, the two-parameter Hubbard model is used. This model is unable to capture the electron–hole asymmetry in the electronic band structure obtained from first principles calculations [25]. Hence, the necessity for a quantitative study, which accounts for the spin degree of freedom in the electronic transport properties of disordered ZGNRs, is of fundamental importance for the development of GNR-based electronic devices.

In this paper, for the first time, we investigate the effect of structural imperfections such as single atom vacancies,

Manuscript received August 23, 2013; revised October 24, 2013; accepted November 6, 2013. Date of publication November 22, 2013; date of current version December 20, 2013. The review of this paper was arranged by Editor J. Knoch.

N. Djavid, K. Khaliji, and S. M. Tabatabaei are with the Department of Electrical and Computer Engineering, University of Tehran, Tehran 14395-515, Iran (e-mail: nimadjavid@ut.ac.ir; kavehkhaliji@ut.ac.ir; s.m.tabatabaei@ut.ac.ir).

M. Pourfath is with the Department of Electrical and Computer Engineering, University of Tehran, Tehran 14395-515, Iran, (e-mail: pourfath@ut.ac.ir) and also with the Institute for Microelectronics, Technische Universität Wien, Gußhausstraße 27–29/E360, A-1040 Wien, Austria (e-mail: pourfath@iue.tuwien.ac.at).

N. Djavid and K. Khaliji equally contributed to this work.

Color versions of one or more of the figures in this paper are available online at http://ieeexplore.ieee.org.

Digital Object Identifier 10.1109/TED.2013.2290773

0018-9383 © 2013 IEEE

line-edge roughness (LER), and substrate-induced potential fluctuations, on the electronic transport in ultranarrow ZGNRs. To model the electronic transport in defected ZGNRs, we have used the nonorthogonal third nearest neighbor mean-field Hubbard model along with the nonequilibrium Green's function (NEGF) formalism. The influence of LER on ZGNRs is investigated for various geometrical and roughness parameters. The effect of potential fluctuations induced by charged impurities located close to or far from the ribbon–substrate interface on the transport properties of ZGNRs is also studied. This paper is organized as follows: After a brief introduction in Section I, the models and numerical methods are explained in Section II. The role of LER, vacancies, and potential fluctuations on the transport properties of ZGNRs are discussed in Section III. Finally, a short summary and concluding remarks are presented in Section IV.

II. Approach

A. Mean-Field Hubbard Model

Adopting the standard convention in categorizing ZGNRs, we have used the notation of N_z-ZGNR, which refers to an ZGNR with N_z zigzag chains across its width. Considering nonorthogonal p_z orbitals as the basis set and employing the mean-field approximation for the Hubbard Hamiltonian, one obtains:

$$H = -\sum_{ij\sigma}\left[t_{ij\sigma}c^{\dagger}_{i\sigma}c_{j\sigma} + H.c.\right] + U\sum_{i}[n_{i\uparrow}\langle n_{i\downarrow}\rangle + n_{i\downarrow}\langle n_{i\uparrow}\rangle - \langle n_{i\uparrow}\rangle\langle n_{i\downarrow}\rangle] \quad (1)$$

where $c^{\dagger}_{i\sigma}$, $c_{i\sigma}$, and $n_{i\sigma}$ are the creation, annihilation, and occupation number operators, respectively, for an electron with spin $\sigma = \uparrow, \downarrow$ in the p_z orbital centered at the ith carbon atom in the ZGNR. $t_{ij\sigma}$ is the hopping parameter for an electron with spin σ between p_z orbitals located at some sites i and j, and U is the on-site Coulomb repulsion parameter for the inclusion of short-range electron–electron interactions. Here, we have adopted the generalized tight-binding model from [25], which not only provides a quantitative consistency with first principles local spin density approximation calculations, but also accurately reproduces the results of first principles transport calculations in the presence of structural imperfections in ZGNRs. The values for the first, second, and third nearest neighbor hopping integrals (overlap matrix elements) are $t_1 = 2.7$ eV, $t_2 = 0.09$ eV, and $t_3 = 0.27$ eV ($s_1 = 0.11$, $s_2 = 0.045$, and $s_3 = 0.065$) and the Hubbard parameter is $U = 2$ eV. The validity of the mean-field approximation for the considered values of U and t_1 is comprehensively verified in [26].

Equation (1) can be decoupled into two spin-dependent Hamiltonians with the diagonal elements of up- or down-spin blocks depending on the mean value of the spin resolved electron density computed as:

$$\langle n_{i\sigma}\rangle = \int dE\ D_{i,\sigma}(E)f(E - E_F) \quad (2)$$

where $D_{i,\sigma}$ is the local density of states (LDOS) with spin σ at some site i and $f(E - E_F)$ is the Fermi function. To calculate the LDOS, the NEGF formalism is employed [27]. The sketch of simulated structure is shown in Fig. 1. Here, the dangling bonds at the edges are assumed to be saturated with hydrogen atoms. Due to the same electronegativity of the carbon and hydrogen, such passivation does not alter the π-electron system of the ZGNR [23], [28]. Indeed, a previous study has shown that the hydrogen terminated edges are realizable employing the hydrogen plasma etching of the GNRs [29]. The channel length is assumed to be 12 nm. Disorders are only applied to the channel and the contacts are assumed to be perfect and semi-infinitely extended. In addition, the electron–electron interaction is accounted for both in the contacts and channel region [25]. The retarded Green's function of the channel can be written as:

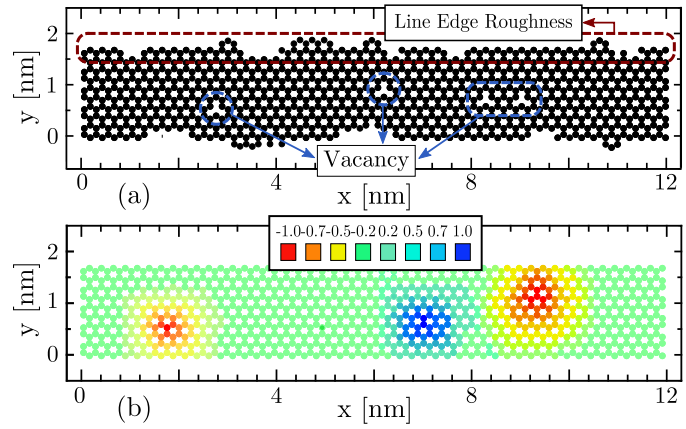

Fig. 1. (a) Schematic diagram of a 12-nm-length ZGNR with vacancies and edge defects. (b) Random sample of normalized potential fluctuations due to the charge impurities in the substrate. For clarity, only the sp^2 carbon atoms belonging to the π-electron system are shown here.

$$G_{\mathrm{ch},\sigma}(E) = \left[(E + i\eta)S_\sigma - H_{\mathrm{ch},\sigma} - \beta^{\dagger}_L g_L \beta_L - \beta_R g_R \beta^{\dagger}_R\right]^{-1} \quad (3)$$

where η is an infinitesimally small quantity. S_σ and $H_{\mathrm{ch},\sigma}$ are the spin-dependent overlap and channel Hamiltonian matrices, respectively. $\beta_{L(R)}$ is the coupling matrix between the channel and left (right) contact and $g_{L(R)}$ is the surface Green's function of the left (right) lead. The latter is efficiently evaluated using the Sancho's iterative scheme [30]. Once $G_{\mathrm{ch},\sigma}$ is obtained, the LDOS in the channel region is calculated as:

$$D_{i,\sigma}(E) = -\frac{1}{\pi}\mathrm{Im}\left[G_{\mathrm{ch},\sigma}(E)S_\sigma\right]_{ii}. \quad (4)$$

Equations (1)–(4) should be solved self-consistently, starting from an antiferromagnetic configuration as the initial guess for the spatial spin densities, until a convergence criterion on the spin densities is fulfilled. It should be mentioned that any initial guess for spin resolved charge densities will lead to similar results if they provide the spin spatial asymmetry needed for achieving the antiferromagnetic solutions [28]. The spin-dependent transmission function of the device is defined as $T_\sigma(E) = \mathrm{Trace}[\Gamma_L G_{\mathrm{ch},\sigma}\Gamma_R G^{\dagger}_{\mathrm{ch},\sigma}]$, where $\Gamma_{L(R)}$ is the broadening function for the left (right) contact and is defined as $\Gamma_L = -2\mathrm{Im}[\beta^{\dagger}_L g_L \beta_L]$ ($\Gamma_R = -2\mathrm{Im}[\beta_R g_R \beta^{\dagger}_R]$). Finally, in the linear response regime, the conductance of the device is

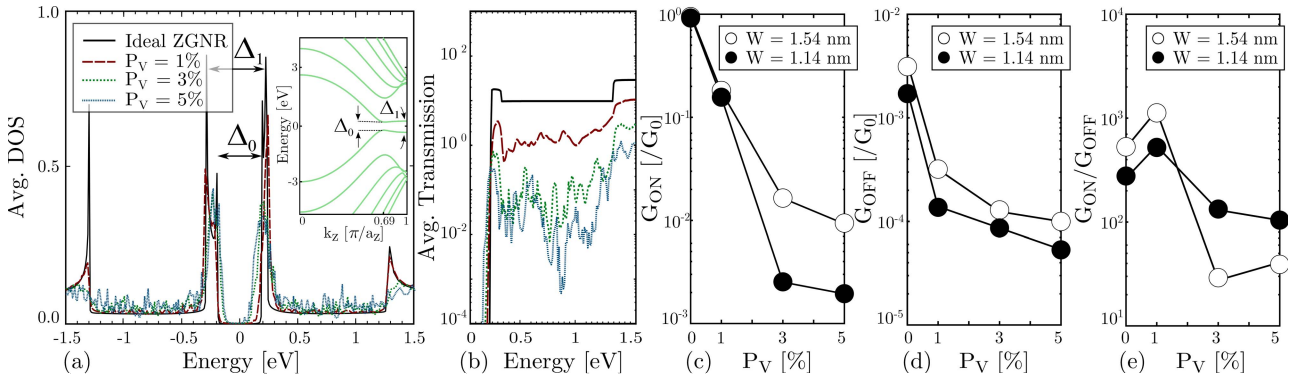

Fig. 2. (a) Normalized average DOS and (b) average transmission probability as a function of energy calculated at various P_V in a 1.14-nm-wide ZGNR. Inset: the electronic band structure of a 1.14-nm-wide ideal ZGNR. (c) and (d) ON- and OFF-state conductances (in units of G_0) and (f) ON/OFF conductance ratio, all plotted as a function of P_V for the two examined widths. The maximum standard deviation of the calculated $\log(G_{ON}/G_{OFF})$ expressed as a percentage of the average value for 1.14- and 1.54-nm-wide ribbons are 25.04 and 24.20, respectively.

calculated as:

$$G = -\sum_{\sigma} G_0 \int dE\ T_\sigma(E) \left(\frac{\partial f}{\partial E}\right)_{E=E_F} \tag{5}$$

with $G_0 = 2e^2/h$. The power supply voltage is set to 0.7 V to meet the required projected V_{DD} for the 12-nm technology node [11]. Hence, the electrostatic influence of the gate on the channel is accounted for by calculating the G_{ON} and G_{OFF} at $E_F = 0.7$ eV and $E_F = 0$ eV, respectively. Room temperature operation is assumed in all simulations.

B. LER, Vacancy, and Substrate Charged Impurities

LER is proved to be the dominant mechanism in degrading the conductance of GNRs narrower than 5 nm [31], [32]. To model LER, we have adopted a relatively realistic statistical approach outlined in [21]. Here, the LER is described by a Gaussian autocorrelation function with no cross-correlation between the edges:

$$R(x_i) = \Delta W^2 \exp\left(\frac{|x_i|}{\Delta L}\right)^2, \qquad x_i = \frac{i\sqrt{3}}{2} a_{cc} \tag{6}$$

where a_{cc} is the carbon–carbon bonding length. ΔW and ΔL are the root mean square (rms) and correlation length (CL) of the roughness fluctuations, respectively. The reason for our choice is that all the experimental reports on the fabrication of extremely scaled GNRs claim they have synthesized nearly perfect edges. Adding a random phase to the Fourier transformation of the autocorrelation function followed by an inverse Fourier transform is employed to generate the random LER profiles in real space.

Single atom vacancies are modeled by randomly removing carbon atoms in the ZGNR to a given percentage, P_V, showing the ratio of the removed to the total number of carbon atoms in the channel. A vacancy at the ith site is modeled by setting the respective hopping parameter in the Hamiltonian to zero.

According to [11], even in high-quality SiO_2 substrates, an impurity concentration as large as 10^{11}cm^{-2} is present. Therefore, once the ZGNR is placed on a substrate, its electronic transport will be affected by the interaction with the charged impurities. The impurities may lead to a small variation of the potential profile either on a scale of a_{cc} or on a scale comparable with a_{cc}. To model these substrate-induced disorders, the widely used random Gaussian potential profile is incorporated as [33]:

$$U(r_i) = \sum_{n=1}^{N_{imp}} U_n \exp\left(-\frac{|r_i - R_n|^2}{2(\xi_n a_{cc})^2}\right) \tag{7}$$

where N_{imp} is the number of impurities centered at an arbitrary point (R_n) within the ZGNR plane. ξ_n and U_n are the CL and amplitude (with realistic values between 0.05 and 0.15 eV [34], [35]) of the nth impurity, respectively.

To capture the general effect of the previously mentioned defects on the electronic transport properties of ZGNRs, for each case of nonidealities, an ensemble average over 50 random samples is carried out to decrease the sample to sample variabilities.

III. Results and Discussion

A. Single Atom Vacancy

In ZGNRs, the states with wave vectors between $2\pi/3a_z$ and $\pi/3a_z$ ($a_z = \sqrt{3}a_{cc}$ is the length of a unit cell of ZGNR) and energies close to the Fermi level, are extended along the ribbon's edges and decay exponentially into the interior parts of the ribbon having wave vector-dependent decay rates. These so-called edge states are fully localized or mostly delocalized if they correspond to the Brillouin zone boundary and $k_z = 2\pi/3a_z$, respectively [7], [8]. In narrow ideal ZGNRs ($N_z < 32$), considering the electron–electron interaction, due to hybridization and consequent bonding–antibonding splitting of mostly delocalized edge states, a width-dependent energy gap (Δ_0) opens up at $k_z \simeq 2\pi/3a_z$ [12] [see the inset of Fig. 2(a)]. Electron–electron interaction in strongly localized edge states leads to a larger energy band splitting (Δ_1) at $k_z = \pi/3a_z$.

Density of states (DOS) at various P_V are shown in Fig. 2(a). Evidently, as P_V increases, while the general trend for DOS in ideal ZGNRs is still preserved, more fluctuations occur in the DOS, and the van Hove singularities are smoothed out. As shown in Fig. 2(b), introducing vacancies uniformly

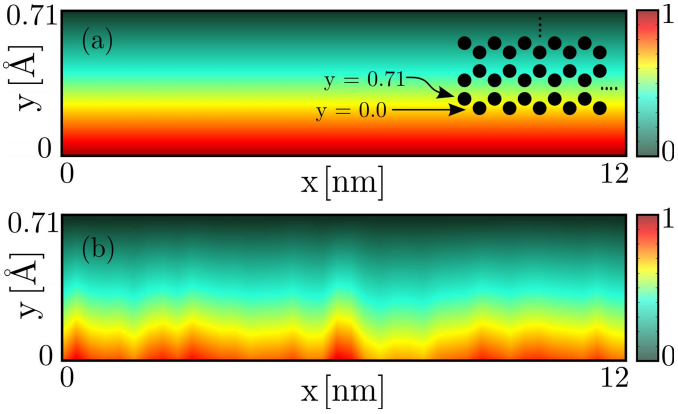

Fig. 3. LDOS for (a) ideal and (b) defected 1.14-nm-wide ZGNR averaged over energy range $0-0.4$ eV. $P_V = 3\%$ in defected ZGNR.

reduces the overall transmission in the whole energy range and in principle should increase the transport gap, defined as the energy range where the transmission probability is smaller than 10^{-2}. However, reducing DOS at the low-energy edge states decreases the corresponding charge density. As a consequence, the electron–electron interaction and the resulting transport gap decreases, diminishing the distinction between Δ_0 and Δ_1. To distinguish the influence of vacant sites from the effects due to the LER, placement of single atom vacancies is prohibited at the edges. Yet, as shown in Fig. 3, due to the ultranarrow widths of the studied structures, such vacant sites can still affect the LDOS profile at the edge carbon atoms. In Fig. 3, an averaging over 0–0.4 eV, the corresponding energy range of the edge states [see Fig. 2(a)], is performed.

ON-, OFF-state conductances and ON/OFF conductance ratio as a function of P_V for the two examined ZGNRs are shown in Fig. 2(c)–(e), respectively. As P_V increases, due to the overall reduction of transmission around $E_F = 0.7$ eV, G_{ON} decreases. Furthermore, the ON-state conductance of wider ZGNRs is less affected when subjected to vacancies. In the presence of vacancies, despite the reduction of the transport gap, OFF-state conductance decreases. To explain this behavior, one should notice that the thermal broadening function ($\partial f/\partial E$) in (5), only encompasses transmission probabilities with energies in a $\Delta E_{\mathrm{eff}} = 0.6$ eV energy range around the Fermi level, which is set to be $E_F = 0$ eV for the OFF-state (ΔE_{eff}, is the effective energy range for the thermal broadening function, namely the energy range where product of averaged transmission probability and $\partial f/\partial E$ is higher than 1% of its maximum value). Since, in narrow ribbons under study, in the 0–0.3 eV energy range, the degradation of the transmission probability is more pronounced than the reduction of the transport gap, [see Fig. 2(b)], the decreasing trend of the OFF-state conductance as a function of P_V can be attributed to the universal reduction of the transmission probability. The trends in ON- and OFF-state conductances should naturally result in a descending ON/OFF conductance ratio versus P_V. However, a maximum at $P_V = 1\%$ is observed, which is attributed to the steeper decrease of the OFF-state conductance compared with the ON-state conductance.

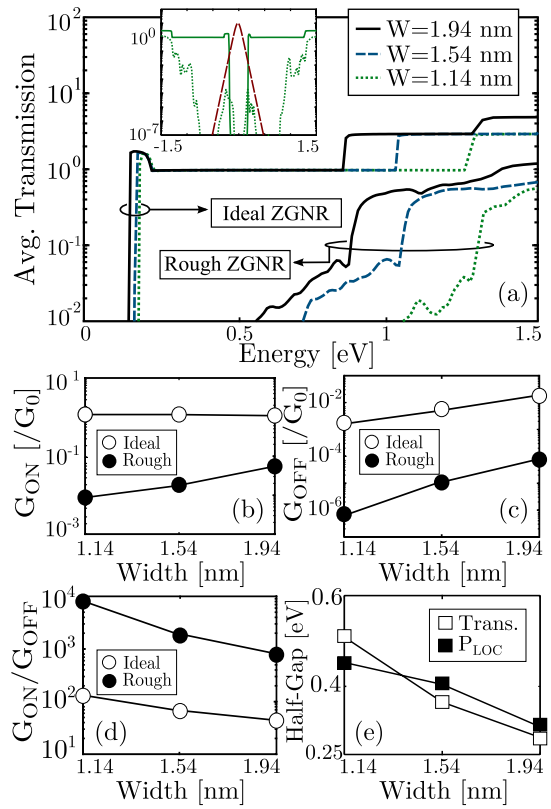

Fig. 4. (a) Average transmission probabilities of perfect and edge-defected ZGNRs at various widths. Inset: the results for 1.14-nm-wide perfect (solid line) and edge-defected (dotted line) ZGNR over a wider interval. Red dashed curve: the thermal broadening function. (b) and (c) ON- and OFF- conductances (in units of G_0) and (d) ON/OFF conductance ratio, all plotted as a function of width for perfect (dashed lines) and edge-defected (solid lines) ZGNRs. (e) Width dependence of the half-transport gap in edge-defected ZGNRs calculated from the transmission probability and P_{LOC}. In all these figures, $\Delta L = 3$ nm and $\Delta W/W = 2\%$. The standard deviation of $\log(G_{\mathrm{ON}}/G_{\mathrm{OFF}})$ given as a percentage of the average value for 1.14-, 1.54-, and 1.94-nm-wide ribbons are 26.97, 23.93, and 21.11, respectively.

B. Line-Edge Roughness

The average transmission probability of perfect and edge-defected ZGNRs at various widths (1–2 nm) are shown in Fig. 4(a). In the presence of LER, the stepwise behavior in the ideal ZGNRs is washed out. Evidently, as the ribbon's width increases, the influence of LER is decreased. Furthermore, as opposed to ZGNRs defected by vacancies where the transmission probability is uniformly suppressed in the whole energy range, in the presence of LER, the degradation is stronger at lower energies. To explain this behavior, one should notice that low energies correspond to the states localized at the edges. Such states are highly sensitive to the relative position of the vacant sites to the edges. Hence, they are severely affected by LER. As shown in the inset of Fig. 4(a), edge-defected ZGNRs have nonzero transmission probabilities in the energy range corresponding to the transport gap of the ideal ribbon [see inset of Fig. 4(a)]. This behavior can be attributed to the reduction in the electron–electron interaction similar to the case previously explained for vacancies. However, due to the much more significant reduction of the transmission probability in the presence of LER, and since we evaluate

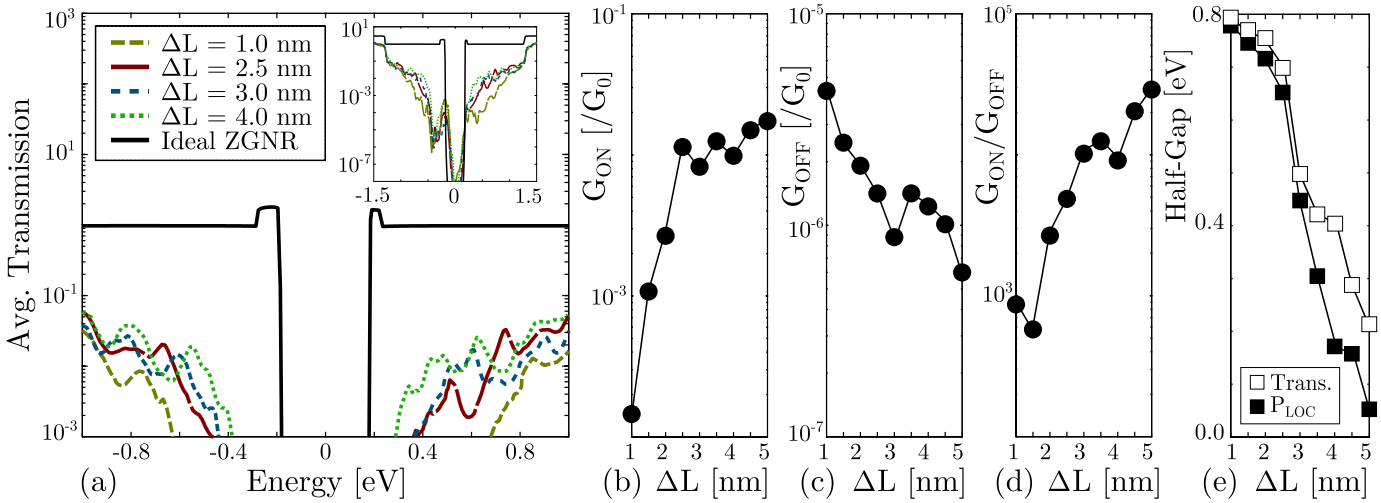

Fig. 5. (a) Average transmission probability as a function of energy at various CLs in edge-defected ZGNRs. Inset: the results over a wider interval. (b) and (c) ON- and OFF-state conductances (in units of G_0). (d) ON/OFF conductance ratio, all plotted as a function of CL. (e) Dependence of the half-transport gap on CL calculated from the transmission probability and P_{LOC}. In all these figures, $\Delta W/W = 2\%$ and $W = 1.14$ nm. The maximum standard deviation of $\log(G_{\mathrm{ON}}/G_{\mathrm{OFF}})$, calculated for various CLs, expressed as a percentage of the average value is equal to 29.76.

the transport gap values at magnitudes of the transmission probability as high as 10^{-2}, one can see that the transport gap in edge-defected ZGNRs is significantly increased compared with the ideal ribbons.

ON-, OFF-state conductances and ON/OFF conductance ratio as a function of width are shown in Fig. 4(b)–(d), respectively. For perfect ZGNRs with widths in the range 1-2 nm, as the ribbon becomes wider, G_{ON} remains constant owing to the fixed value of the transmission probability around $E_F = 0.7$ eV and G_{OFF} increases due to the reduction of the bandgap. In the presence of LER, the aforementioned trend for G_{OFF} as a function of width is preserved. Furthermore, compared with ideal ZGNRs and ribbons defected by vacancies, OFF-state conductances have smaller values. Considering G_{ON}, it can be seen that the ON-state conductance of the edge-defected ZGNRs are smaller than that of ideal ribbons and the reduction is less pronounced when the ribbons width is increased. It should be mentioned that in Fig. 4, defining the relative roughness amplitude as $\Delta W/W$, the ribbons with different widths are compared when they are exposed to the same amount of roughness compared to their width. This approach has been previously adopted for AGNRs in [21]. Furthermore, it can be easily concluded that if the ascending trend of G_{ON} and G_{OFF} are present in the case of fixed $\Delta W/W$, they will be surely present in the case where ΔW is kept constant.

To study the role of edge defects on the transport gap of GNRs, mobility edge theory can be applied [20], [34]. This model employs an LDOS-based parameter, which quantitatively describes the degree of uniformity in the spatial distribution of the DOS along the transport direction:

$$P_{\mathrm{LOC}}(E) = \left(N_\eta(E)/N_{\mathrm{tot}} - N_R\right) \times 100 \tag{8}$$

where N_{tot} is the total number of atoms in the perfect channel, N_R is the number of removed atoms, and N_η is the number of atomic sites with DOS higher than 5% of the maximum DOS at that energy. Previously, it has been shown that mobility edge theory is unable to predict the transport gap in extremely scaled AGNRs [20]. In this paper, the validity of this model in edge-defected ultranarrow ZGNRs is investigated. The width dependence of the half-gap extracted from the transmission probability and P_{LOC} (defined as energy range where P_{LOC} is less than 50%) is shown in Fig. 4(e). While edge-defected AGNRs exhibit strongly localized nonzero DOS in the transport gap [20], electron–electron interactions in edge-defected ZGNRs prevent such localized states to be formed in the transport gap energy range. Although such states in edge-defected ZGNRs are localized at the edges, they are extended along the ribbon's length connecting the source and drain regions. This accompanied by the destructive influence of the LER on localized edge states lead to a consistency between P_{LOC}- and transmission-based transport gap values.

Fig. 5(a) shows that the transmission probability decreases as the CL is reduced. Clearly, the reduction is more pronounced at lower energies. As a result, one would expect both ON- and OFF-conductances decrease as CL is reduced. While this is indeed the case for G_{ON} [see Fig. 5(b)], G_{OFF} increases as CL is shrunk [see Fig. 5(c)]. This behavior is related to the increase of the transmission probability in the bandgap energy range of the ideal ribbon at very short CLs [see the inset of Fig. 5(a)]. Therefore, with increasing CL, the ON/OFF conductance ratio is increased [see Fig. 5(d)]. Fig. 5(e) compares the half-gap obtained by P_{LOC} and transmission probability. The results show that despite the discrepancy at long CLs, P_{LOC} can appropriately predict the transmission-based transport gaps at short CLs or in the presence of rough LER profiles.

The average transmission probability as a function of energy and relative roughness amplitude is shown in Fig. 6(a). Similar to the case where ΔL is decreased, with increasing $\Delta W/W$, the transmission probability is reduced in the whole energy range. The reduction, however, is much more pronounced at higher energies compared with the case where CL is short, suggesting that the corresponding bulk states are more affected by relative roughness amplitude rather than CL of the LER profile. Fig. 6(b) and (c) shows ON- and OFF-state

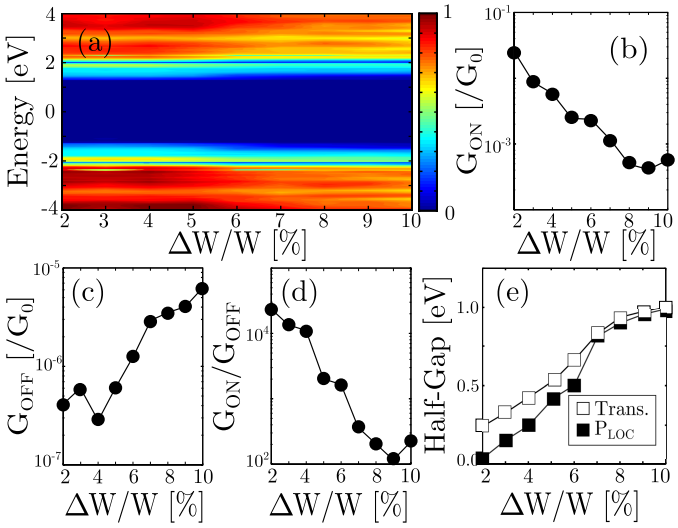

Fig. 6. (a) Average transmission probability as a function of energy and relative roughness amplitude in edge-defected ZGNRs. (b) and (c) ON- and OFF-state conductances (in units of G_0). (d) ON/OFF conductance ratio, all plotted as a function of relative roughness amplitude. (e) Dependence of the half-transport gap on the relative roughness amplitude calculated from the transmission probability and P_{LOC}. In all these figures, $\Delta L = 5$ nm and $W = 1.14$ nm. The maximum standard deviation of $\log(G_{\mathrm{ON}}/G_{\mathrm{OFF}})$, calculated for various values of $\Delta W/W$, given as a percentage of the average value is equal to 31.03.

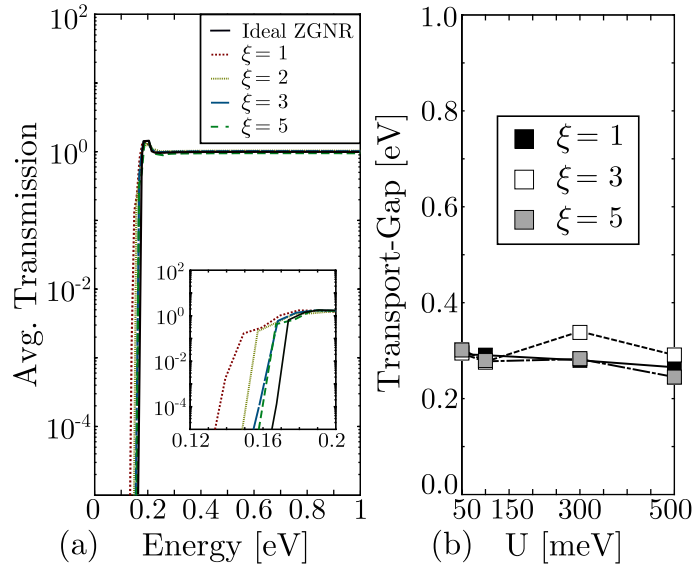

Fig. 7. (a) Average transmission probability of a 1.14-nm-wide ZGNR for $U = 0.3$ eV and various magnitudes of ξ. (b) Transport gap of a 1.14-nm-wide ZGNR as a function of U for different values of ξ.

conductances at various $\Delta W/W$ for a 1.14-nm-wide ribbon, respectively. Accordingly, as $\Delta W/W$ increases, G_{ON} (G_{OFF}) decreases (increases). As shown in Fig. 6(d), P_{LOC}-based transport gaps for large values of $\Delta W/W$ are in good agreement with the transmission-based gaps. These results can be explained in the same manner as that of CL.

C. Substrate Charged Impurities

The average transmission probability of a 1.14-nm-wide ZGNR as a function of ξ for $U = 0.3$ eV is shown in Fig. 7(a). Evidently, substrate impurities have negligible influence on the transmission probability, regardless of ξ or their relative distance from the ZGNR plane. As shown in the inset of Fig. 7(a), as ξ increases—corresponding to impurities being located closer to the ribbon's plane—transport gap is slightly reduced. Hence, considering realistic values of fluctuation amplitude, which are well below $U = 0.3$ eV (50 meV $\leq U \leq$ 150 meV), variation of ξ has negligible impact on the transmission probability. To explain the results, it should be mentioned that in the presence of charged impurities, the diagonal elements of the channel Hamiltonian are remained relatively unchanged compared with the ideal ZGNR. In other words, on-site potentials are more influenced by the on-site Coulomb repulsion term than by the associated potential perturbation terms due to substrate charged impurities. This results in a strong robustness of the electronic transport properties of ZGNR in comparison with its armchair counterpart, where the ground state is nonmagnetic and on-site potentials are initially assumed to be zero. As a result in AGNRs, even realistic values of fluctuation amplitudes can affect the DOS and transmission probability [20]. Transport gap as a function of disorder amplitude is shown in Fig. 7(b). It is clear that even for relatively large values of U, transport gap is weakly affected. Our results show that irrespective of the strength of charged impurities, ON- and OFF-state conductances are negligibly affected compared with the ideal ribbons. This can be readily inferred from the 3.12% maximum standard deviation of ON/OFF conductance ratio for potential fluctuations induced by the charged impurities.

IV. Conclusion

The role of LER, single atom vacancies, and potential fluctuations due to the substrate charged impurities on the electronic transport properties of ultranarrow ZGNRs has been investigated in this paper. Mean-field Hubbard model with nonorthogonal basis set considering up to third nearest neighbor interactions along with the NEGF formalism has been employed to evaluate the results.

In contrast to ultranarrow AGNRs, our calculations revealed that introducing vacancies can reduce the transport gap in ZGNRs. We found that in the presence of vacancies, despite the transport gap is reduced, the OFF-state conductance is decreased due to the reduction of the transmission probability around the Fermi energy level.

With our results, LER significantly suppresses the transmission probability at low energies, resulting in an increase in the transport gap as the degree of roughness in the edge profile increases. Hence, as CL (rms) decreases (increases), ON- and OFF-state conductances tend to decrease and increase, respectively. Moreover, by incorporating an LDOS-based parameter model, we showed that the mobility edge theory can accurately assess the transport gap in rough edged ultranarrow ZGNRs, in contrast to the case for extremely scaled edge-defected AGNRs where this model fails to predict the transport gap [20].

Employing the widely used random Gaussian potential profile, we have shown that potential fluctuations have a negligible influence on the transport properties of ZGNRs in comparison

with their armchair counterparts, implying superior robustness of ZGNRs in the presence of potential fluctuations.

In conclusion, our results demonstrate the significant influence of the structural disorders on the electronic transport properties of technologically relevant extremely scaled ribbons, emphasizing the role of nonidealities in the performance characteristics of realistic devices. Our work for ultranarrow ZGNRs along with a similar study for AGNRs presented in [20], comprehensively unfolds the effect of structural imperfections on the electronic transport properties of GNRs at extremely scaled dimensions.

REFERENCES

[1] K. Novoselov, A. Geim, and S. Morozov, "Electric field effect in atomically thin carbon films," *Science*, vol. 306, no. 5696, pp. 666–669, 2004.

[2] X. Li, X. Wang, L. Zhang, S. Lee, and H. Dai, "Chemically derived, ultrasmooth graphene nanoribbon semiconductors," *Science*, vol. 319, no. 5867, pp. 1229–1232, Feb. 2008.

[3] J. Cai, P. Ruffieux, R. Jaafar, M. Bieri, T. Braun, S. Blankenburg, *et al.*, "Atomically precise bottom-up fabrication of graphene nanoribbons," *Nature*, vol. 466, no. 7305, pp. 470–473, 2010.

[4] S. Blankenburg, J. Cai, P. Ruffieux, R. Jaafar, D. Passerone, X. Feng, *et al.*, "Intra-ribbon heterojunction formation in ultranarrow graphene nanoribbons," *ACS Nano*, vol. 6, no. 3, pp. 2020–2025, 2012.

[5] Y. Kobayashi, K.-I. Fukui, T. Enoki, and K. Kusakabe, "Edge state on hydrogen-terminated graphite edges investigated by scanning tunneling microscopy," *Phys. Rev. B*, vol. 73, no. 12, pp. 125415-1–125415-3, 2006.

[6] Y. Kobayashi, K.-I. Fukui, T. Enoki, K. Kusakabe, and Y. Kaburagi, "Observation of zigzag and armchair edges of graphite using scanning tunneling microscopy and spectroscopy," *Phys. Rev. B*, vol. 71, no. 19, pp. 193406-1–193406-4, 2005.

[7] K. Nakada, M. Fujita, G. Dresselhaus, and M. S. Dresselhaus, "Edge state in graphene ribbons: Nanometer size effect and edge shape dependence," *Phys. Rev. Lett.*, vol. 54, no. 24, pp. 17954–17961, 1996.

[8] M. Fujita, K. Wakabayashi, K. Nakada, and K. Kusakabe, "Peculiar localized state at zigzag graphite edge," *J. Phys. Soc.*, vol. 65, no. 7, pp. 1920–1923, 1996.

[9] Y.-W. Son, M. L. Cohen, and S. G. Louie, "Half-metallic graphene nanoribbons," *Nature*, vol. 444, no. 7117, pp. 347–349, 2006.

[10] J. Bai, R. Cheng, F. Xiu, L. Liao, M. Wang, A. Shailos, *et al.*, "Very large magnetoresistance in graphene nanoribbons," *Nature Nanotechnol.*, vol. 5, no. 9, pp. 655–659, 2010.

[11] (2011). *International Technology Roadmap for Semiconductors* [Online]. Available: http://www.itrs.net

[12] Y.-W. Son, M. L. Cohen, and S. G. Louie, "Energy gaps in graphene nanoribbons," *Phys. Rev. Lett.*, vol. 97, no. 21, pp. 216803-1–216803-4, Nov. 2006.

[13] D. A. Areshkin, D. Gunlycke, and C. T. White, "Ballistic transport in graphene nanostrips in the presence of disorder: Importance of edge effects," *Nano Lett.*, vol. 7, no. 1, pp. 204–210, 2007.

[14] D. Gunlycke, D. A. Areshkin, and C. T. White, "Semiconducting graphene nanostrips with edge disorder," *Appl. Phys. Lett.*, vol. 90, no. 14, pp. 142104-1–142104-6, 2007.

[15] Y. Yoon and J. Guo, "Effect of edge roughness in graphene nanoribbon transistors," *Appl. Phys. Lett.*, vol. 91, no. 7, pp. 073103-1–073103-3, 2007.

[16] M. Evaldsson, I. V. Zozoulenko, H. Xu, and T. Heinzel, "Edge disorder induced Anderson localization and conduction gap in graphene nanoribbons," *Phys. Rev. B*, vol. 78, no. 1, pp. 161407-1–161407-4, 2008.

[17] E. R. Mucciolo, A. H. Castro Neto, and C. H. Lewenkopf, "Conductance quantization and transport gaps in disordered graphene nanoribbons," *Phys. Rev. B*, vol. 79, no. 7, pp. 075407-1–075407-5, 2009.

[18] A. Yazdanpanah, M. Pourfath, M. Fathipour, and H. Kosina, "Device performance of graphene nanoribbon field effect transistors in the presence of line-edge roughness," *IEEE Trans. Electron Devices*, vol. 59, no. 12, pp. 3527–3532, Dec. 2012.

[19] J. J. Palacios, J. Fernández-Rossier, and L. Brey, "Vacancy-induced magnetism in graphene and graphene ribbons," *Phys. Rev. B*, vol. 77, no. 19, pp. 195428-1–195428-3, 2008.

[20] M. Poljak, S. Member, E. B. Song, M. Wang, T. Suligoj, and K. L. Wang, "Influence of edge defects, vacancies, and potential fluctuations on transport properties of extremely scaled graphene nanoribbons," *IEEE Trans. Electron Devices*, vol. 59, no. 12, pp. 3231–3238, Dec. 2012.

[21] A. Yazdanpanah, M. Pourfath, M. Fathipour, H. Kosina, and S. Selberherr, "A numerical study of line-edge roughness scattering in graphene nanoribbons," *IEEE Trans. Electron Devices*, vol. 59, no. 2, pp. 433–440, Feb. 2012.

[22] Y. Sui, T. Low, M. Lundstrom, and J. Appenzeller, "Signatures of disorder in the minimum conductivity of graphene," *Nano Lett.*, vol. 11, no. 3, pp. 1319–1322, 2011.

[23] O. V. Yazyev, "Emergence of magnetism in graphene materials and nanostructures," *Rep. Progr. Phys.*, vol. 73, no. 5, pp. 056501-1–056501-3, 2010.

[24] H. Kumazaki and D. S. Hirashima, "Spin polarized transport on zigzag graphene nanoribbon with a single defect," *J. Phys. Soc. Jpn.*, vol. 78, no. 9, pp. 094701-1–094701-6, 2009.

[25] Y. Hancock, A. Uppstu, K. Saloriutta, A. Harju, and M. J. Puska, "Generalized tight-binding transport model for graphene nanoribbon-based systems," *Phys. Rev. B*, vol. 81, no. 24, pp. 245402-1–245402-6, 2010.

[26] H. Feldner, Z. Y. Meng, A. Honecker, D. Cabra, S. Wessel, and F. F. Assaad, "Magnetism of finite graphene samples: Mean-field theory compared with exact diagonalization and quantum Monte Carlo simulations," *Phys. Rev. B*, vol. 81, no. 11, pp. 115416-1–115416-5, 2010.

[27] M. P. Anantram and A. Svizhenko, "Multidimensional modelling of nanotransistors," *IEEE Trans. Electron Devices*, vol. 54, no. 9, pp. 2100–2115, Sep. 2007.

[28] B. Sanyal and O. Eriksson, *Advanced Functional Materials: A Perspective from theory and Experiment*. New York, NY, USA: Elsevier, 2012.

[29] X. Zhang, O. V. Yazyev, J. Feng, L. Xie, C. Tao, Y.-C. Chen, *et al.*, "Experimentally controlling the edge termination of graphene nanoribbons," *ACS Nano*, vol. 7, no. 1, pp. 198–202, 2013.

[30] M. P. L. Sancho, J. M. L. Rubio, and L. Rubio, "Highly convergent schemes for the calculation of bulk and surface green functions," *J. Phys. F, Metal Phys.*, vol. 15, no. 4, pp. 851–858, 1985.

[31] R. Murali, "Impact of size effect on graphene nanoribbon transport," *IEEE Electron Device Lett.*, vol. 31, no. 3, pp. 237–239, Mar. 2010.

[32] T. Fang, A. Konar, H. Xingi, and D. Jena, "Mobility in semiconducting graphene nanoribbons: Phonon, impurity, and edge roughness scattering," *Phys. Rev. B*, vol. 78, no. 20, pp. 205403-1–205403-8, 2008.

[33] C. Lewenkopf, E. Mucciolo, and A. Castro Neto, "Numerical studies of conductivity and Fano factor in disordered graphene," *Phys. Rev. B*, vol. 77, no. 8, pp. 081410-1–081410-1, 2008.

[34] J. Martin, N. Akerman, G. Ulbricht, T. Lohmann, J. H. Smet, K. von Klitzing, *et al.*, "Observation of electron-hole puddles in graphene using a scanning single-electron transistor," *Nature Phys.*, vol. 4, no. 2, pp. 144–148, 2008.

[35] C. Stampfer, J. Güttinger, S. Hellmüller, F. Molitor, K. Ensslin, and T. Ihn, "Energy gaps in etched graphene nanoribbons," *Phys. Rev. Lett.*, vol. 102, no. 5, pp. 056403-1–056403-4, 2009.

[36] D. Querlioz, Y. Apertet, A. Valentin, K. Huet, A. Bournel, S. Galdin-Retailleau, *et al.*, "Suppression of the orientation effects on bandgap in graphene nanoribbons in the presence of edge disorder," *Appl. Phys. Lett.*, vol. 92, no. 4, pp. 042108-1–042108-3, 2008.

Authors' photographs and biographies not available at the time of publication.